Integrated Metasurfaces for Advanced Solid-State-Lighting

Integrated Metasurfaces for Advanced Solid-State-Lighting

Toni Lopez[a], Mohamed S. Abdelkhalik[b], Xavi Garcia[a], Jaime Gomez Rivas[b], Luke Gordon[c], Hisashi Masui[c], Marcel Bohmer[a]

[a] Lumileds Germany GmbH, Philipsstraße 8, 52068 Aachen, Germany; [b] Department of Applied Physics and Science Education, and Eindhoven Hendrik Casimir Institute, P.O. Box 513, 5600 MB Eindhoven, The Netherlands; [c] Lumileds, 370 W Trimble Rd, San Jose, CA 95131 United States

ABSTRACT

Light-Emitting Diodes (LEDs) exhibit a typical Lambertian emission, usually requiring reshaping by means of secondary optics. We review the potential of various integrated photonic architectures to address the demand for system miniaturization and high efficiency in emerging applications. Photonic structures that can be potentially integrated in LED devices include metalenses, photonic crystals and reflective metasurfaces. We embed periodic nanoantennas in InGaN/GaN multi-quantum well (MQW) LEDs to control their far-field emission directionality and enhance collection efficiency. We propose exploiting mechanisms such as surface lattice resonances, which rely on the near-field coupling between the quantum wells and the nanoantenna array. Multiple experimental and modeling studies demonstrate the benefits and challenges of optimized integrated metasurfaces to enable efficient SSL sources without the need of bulky secondary optics for directional beam control.

1. MOTIVATION

Emerging applications such as wearable smart watches, augmented reality (AR) glasses and related mobile devices are pushing the boundaries of the display industry wherein, among numerous other requirements, power consumption and compactness are key concerns. With respect to SSL sources, inorganic LED technology is correspondingly evolving to meet these demands. Examples include adaptive LEDs for local dimming in AR displays [1], and recent progress in microLEDs with regards to materials, device performance, architectures, and reliability [2]. Nonetheless, the following challenges continue to gain much attention:

(1) The angular emission of LED sources remains fundamentally Lambertian unless extrinsic or intrinsic leverage mechanisms are introduced to steer the radiation profile. The most commonly used extrinsic means is that offered by conventional collimating lenses, which collect light at the cost of area increase as dictated by the conservation of etendue. This limitation has been extensively studied to quantify the minimum volume size achievable in designs (e.g. reference [3]).
(2) The light extraction efficiency (ExE) decreases with pixel size. The severity of this trade-off has been recognized as the dimension of the pixels shrink below 100µm, to the extent that ExE can become the single greatest efficiency limitation in microLED emitters [2].

There are two main reasons to be concerned about ExE. On the one hand, side-walls that optically isolate pixels tend to be absorbing. On the other hand, traditional methods to boost ExE in millimeter-size LEDs may no longer be attainable in microLED architectures suitable for mass manufacturing. Such is the case of conventional patterned sapphire substrates (PSS) [4] or photoelectrochemical etching [5] techniques for texturing the light emitting surface (LES) of the LED.

Figure 1 qualitatively summarizes the two aforementioned performance trends as a function of pixel size. Note however the non-monotonic behavior at very small pixel sizes, where the lateral dimension becomes comparable to the epitaxial layer thickness. Under such geometrical conditions, the mesa side-wall arises as an intrinsic leverage mechanism to both recover ExE and steer the angular radiation pattern. This involves process optimizations for engineering side-wall angles with preferential cup shapes that favor light outcoupling.

Smart Photonic and Optoelectronic Integrated Circuits 2024, edited by
Sailing He, Laurent Vivien, Proc. of SPIE Vol. 12890, 1289002
 · 0277-786X · doi: 10.1117/12.2692603

Figure 2 further illustrates the shift from pixel structures featuring PSS based textured LES, such as those used in automotive front lighting, to architectures better suited for mass manufacturing smaller pixel sizes. Below 20µm, alternative process flows may introduce the use of transparent conductive oxide (TCO) layers in order to inject current into the semiconductor from the LEA. While this may offer architectural advantages to achieve high-density pixel arrays, it can certainly limit the ability to process textured LEA for optimal light outcoupling.

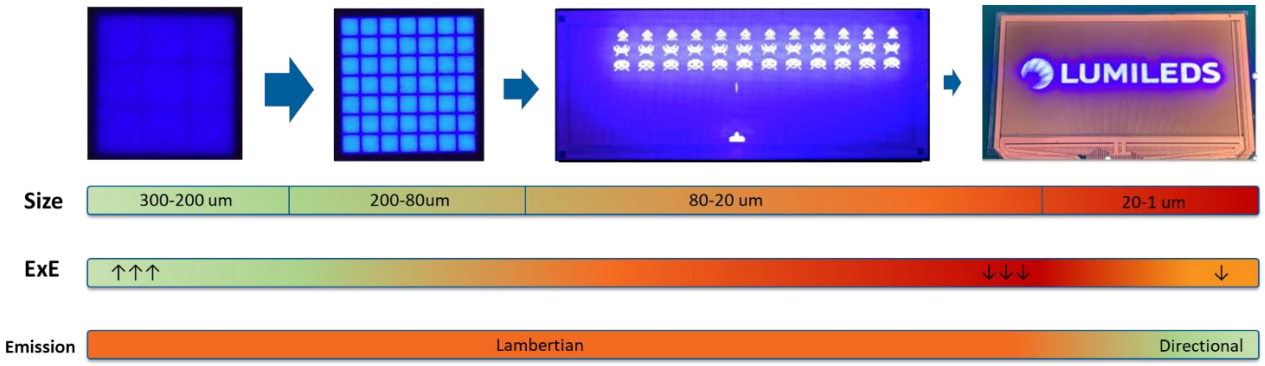

Figure 1. ExE and angular emission characteristics as pixel size shrinks. From left to right, we illustrate adaptive LED sources for local dimming in AR displays showing the largest pixel segments, high power arrays for Automotive front lighting with pixels sizes of 50µm, to direct-view micro-displays [6] with target pixel sizes below 20µm.

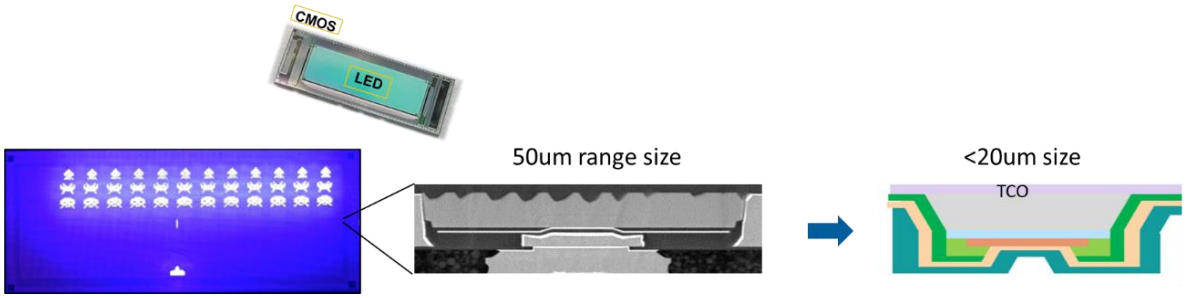

Figure 2. Pixel architectures may vary with size requirements. Pixels smaller than 20µm may lack textured LEA for optimal light outcoupling.

Consequently, we propose to address these challenges with the aid of photonics and device integration capabilities. Within the scope of this work, we consider the photonic structures presented in Figure 3, which we describe in the following sections.

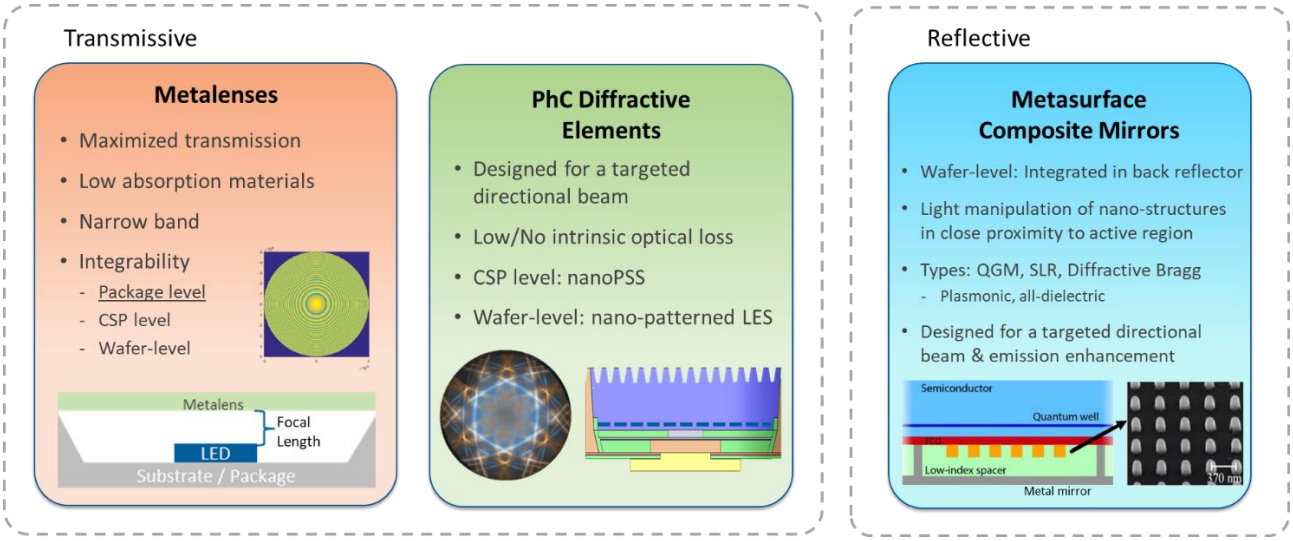

Figure 3. Selected nanostructures for integration in LED devices.

2. METALENSES

We consider metalenses as potential integral part of packaged solutions such as mid-power color LEDs [7]. These packages could accommodate millimeter size planar metalenses designed with focal distances in the range of 1mm. The advantages in volume size and compactness relative to conventional lenses are apparent by comparing the schemes in Figure 4.

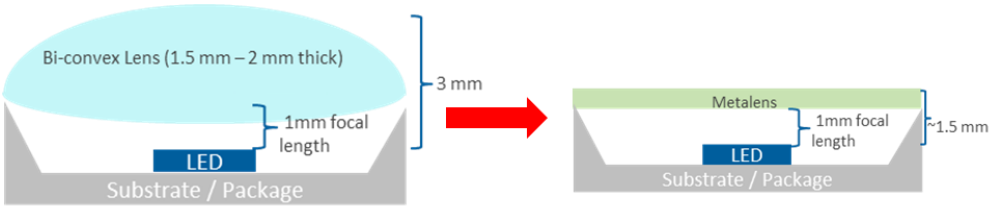

Figure 4. Package level solution integrating a metalens structure patterned on a submillimeter thick transparent substrate.

A complete assessment of this concept must include a performance benchmark against traditional lenses in terms of transmission efficiency. To carry out this task, we completed the following development steps:

- Design phase: The optimization process of large area metalens devices involves the analysis of a large variety of beam benders, which must be studied by means of wave optics tools at its fundamental level, i.e. the meta-atom, and then conveniently transformed into a behavioral model component for large scale Montecarlo optical ray tracing. Efforts in the development of this advanced multiscale modeling technique are being made by major software companies today. The new tools are expected to advance the optical design of modern optical systems as metalens components penetrate ubiquitously in the industry. With our available software tools and custom methods tailored to LED device design and analysis, we completed various metalens designs of sizes up to 5mm, especially suitable to project adaptive LED emitters of 3x3 array segments [1].

- Fabrication phase: We worked with our partner Moxtek, Inc. to fabricate, test, and verify samples of various diameter dimensions processed on glass substrates, which could be tailored for package integration resulting in submillimeter thick metalens devices. In these photonic structures, the basic constituents of the meta-atoms were chosen to be high aspect ratio micro-pillars of high-refractive-index material arranged to steer the phase front of the incoming radiation.

- Characterization phase: Next, we conducted a series of experiments to obtain the transmission and reflection characteristics of the proposed designs. At this stage we could further validate model projections as shown in the transmission data of Figure 5. These results demonstrate that 5mm diameter metalenses with 1.8mm focal length can transmit over 90% of the light at wavelengths longer than 500nm and near normal incidence. In the blue range, however, the transmission is limited to the range of 70%-80%. Reflection measurements were setup such as to represent the multiple scattering reflections between the package surface around the LED chip and the metalens surface that light will experience in the scheme of Figure 4. Accordingly, the grey curve of Figure 6 shows the reflectivity of a collimated broadband beam incident on the metalens lying on a highly reflective and scattering material (i.e. Spectralon®). These results correlate well with the estimated package efficiencies for each color, which are expressed relative to the performance of a conventional collection lens extracted from a Vuzix Blade Light Engine. To obtain these quantities, we carried out total flux measurements using direct-color LED sources located at the entrance port of an integrating sphere while allowing interposing the lens devices in close proximity to the source. The efficiency results are shown in Figure 6 along with a comparison of the measured spectral power levels transmitted through each corresponding lens. Thus, we consistently show with these tests that the efficiency of metalens devices remains a challenge, particularly in the blue spectral range. This demands further improvements in material quality and transparency in the visible band.

- Prototyping: In this last phase, we demonstrate the correct functionality of the metalens to focus light as it gets transmitted. The demonstration is carried out with an adaptive LED emitter of 3x3 array segments individually addressable. As expected, the image of the emitter is projected with the presence of the metalens. Two different on-pixel configurations show the device's ability to effectively focus the generated light of a close-by distributed source.

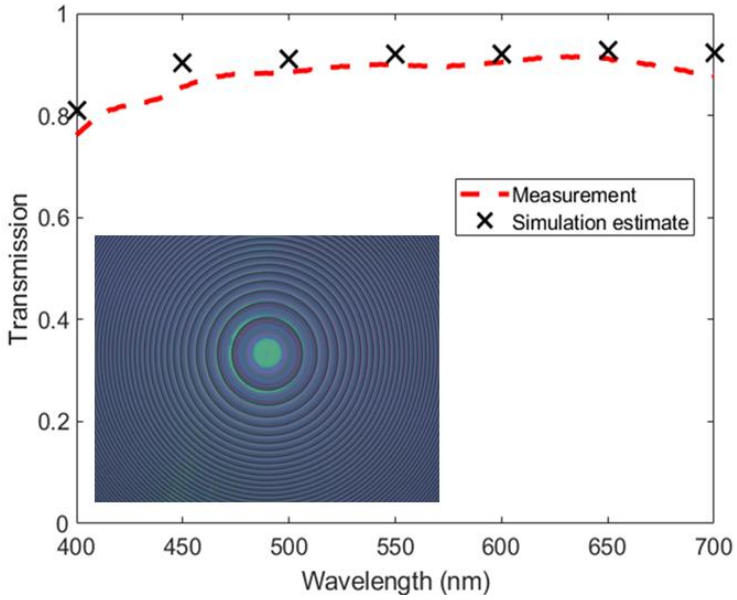

Figure 5. Spectral transmission characteristics of a 5mm diameter metalenses with 1.8mm focal length. The inset microscope image depicts the central area of the metalens sample under investigation.

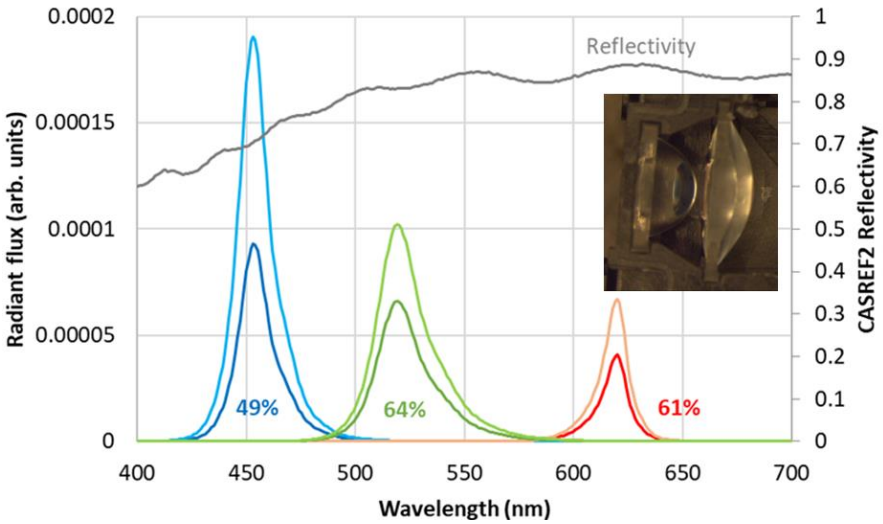

Figure 6. Reflectivity of a collimated broadband beam incident (near normal) on the metalens lying on a highly reflective and scattering material (Spectralon® reference). Blue, green, and red spectral lines compare the total flux transmitted through the metalens and a reference collection lens extracted from a Vuzix Blade Light Engine (see inset image) for three different direct-color LEDs. The percentage quantities refer to the metalens performance relative to that of the reference lens design.

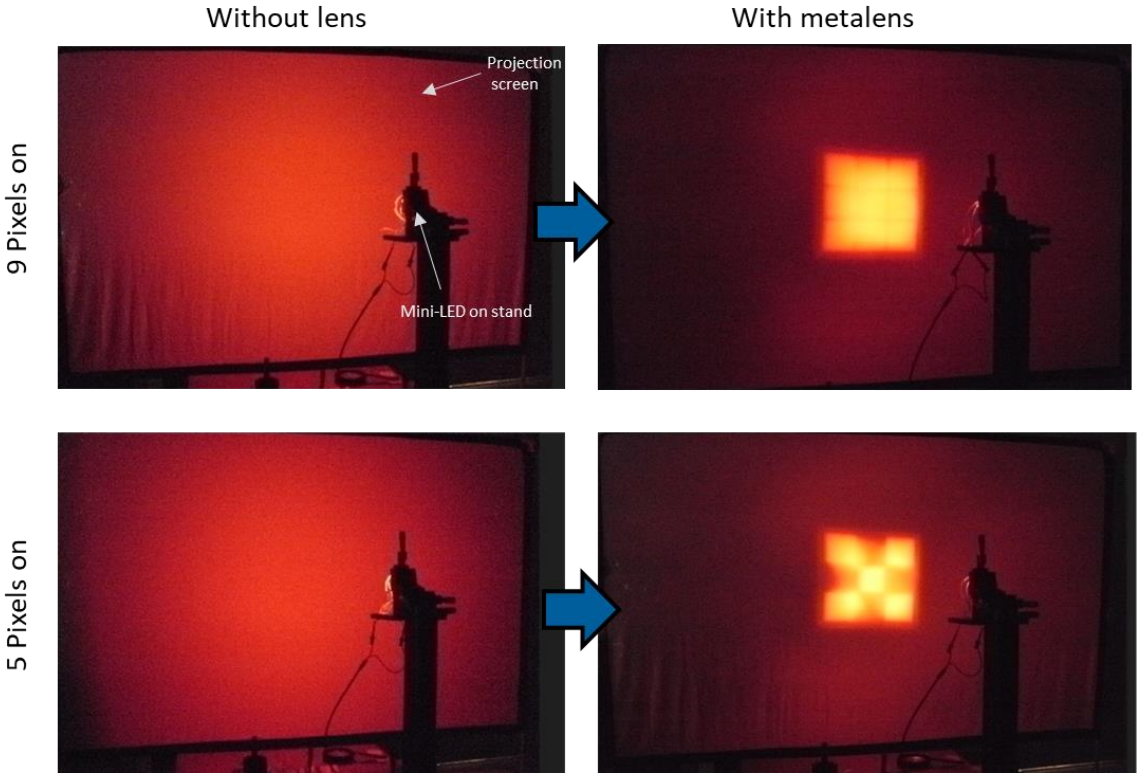

Figure 7. Demonstration setup employing an adaptive red LED emitter of a 3x3 array of 200µm segments individually addressable, a metalens, and a projection wall. Image of the emitter is clearly projected with the presence of the metalens. Two different on-pixel configurations show the device's ability to focus the light of a close-by distributed light source.

3. PHOTONIC CRYSTALS AND DIFFRACTIVE ELEMENTS

The second selected devices from Figure 3 have been extensively studied in the past as decoupling photonic structures that can boost LED efficiency as well as achieve angular emission control. Interesting examples include the work of Wierer [8]-[9].

In reference [8], the proposed resonant cavity LED is designed such that the supported guided modes are coupled to photonic crystal Bloch modes. In addition to obtaining strong beaming capabilities, the resulting structure allows tailoring the Purcell effect, thus enhancing spontaneous emission. Authors estimate up to 73% ExE into air. The key challenge of this proposal is that the epitaxial layer must be extremely thin for efficient mode coupling. Furthermore, efficient resonant-cavity (RC) LEDs require well-controlled submicrometer epitaxial thicknesses, which severely compromises the industrial viability of this architecture.

In reference [9], photonic crystal structures are processed on the LES of conventionally thicker epitaxial layers. This alone represents a major advantage from the view point of industrialization feasibility in contrast to RC-LEDs. Regardless of the corresponding disadvantage in mode volume size increase of this proposal, significant forward-beaming effects and ExE gains are experimentally demonstrated. Nonetheless, the proposed process flow is challenged by the need to grow epitaxial tunnel junctions, the subject of which still remains to this day an intensive area of research in III-V semiconductors.

A more recent and perhaps more viable implementation of diffractive nanostructures is the use of PSS growth with nano-scale features as opposed to the more conventional micron-size textures [10]. Periodic nano-scale motheye-like features can be optimized to significantly steer the angular radiation profile. This is depicted in the simulation results of Figure 9 taking as example the microLED design of Figure 8. As shown, modeling estimates 15% flux gains for 20deg half-cone angle collection, which is comparable to the beam steering capabilities demonstrated in [9]. In the proposed design, optimized periodic structures have hexagonal lattice sizes of 200-500nm and feature heights of 200nm-500nm. The motheye-like shape is shown in Figure 8. It is important to note that the obtained flux gains at narrow collection angles translate into net ExE losses in relation to micron-size PSS-based devices [11].

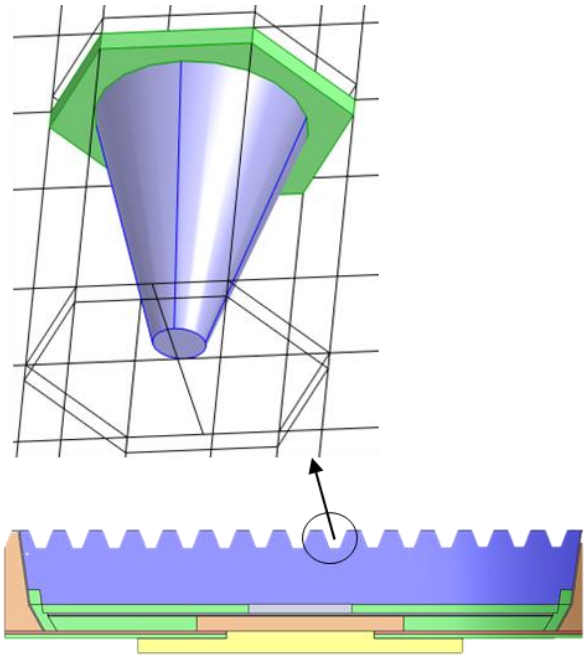

Figure 8. Pixel structure corresponding to a microLED array for automotive front lighting. LES textures represent nano-scale PSS features after sapphire removal (e.g. by a laser lift-off process).

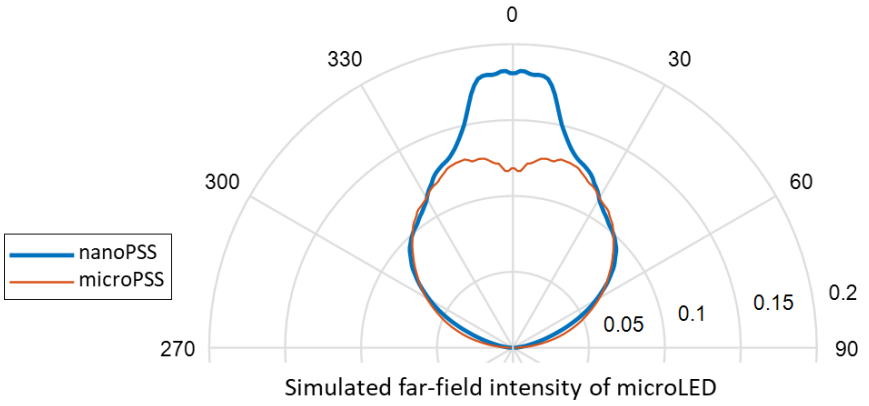

Figure 9. Simulation comparison of angular radiation profiles using both micro-scale and nano-scale PSS textures at the LES of the microLED structure from Figure 8.

4. METASURFACE COMPOSITE MIRRORS

The previous two approaches from Figure 3 are transmission mode based structures with little to no influence to the local density of states (LDOS) as long as the photonic layers are located far away from the active region of the LED. The following structures tackle the problem at the source by influencing the spontaneous radiation of the MQWs typically in near proximity to the mirror reflector deposited on the p-doped GaN layer surface. Unlike other recent studies [12], this is achieved with the prerequisite of preventing epitaxial layer etching and the consequent risk of active region damage and/or deterioration of the emitter performance (e.g. reliability, non-radiative channels, etc.).

It has been widely recognized that simple reflectors such as planar metals, can strongly alter far-field radiation while boosting internal quantum efficiency (IQE) by Purcell enhancement in LED cavities [13]. More recently, LED structures have evolved towards more complex mirror reflectors consisting of composite planar layers such as TCO, dielectric distributed Bragg reflectors (DBR), and metal films. The added complexity is primarily justified by superior reflectance leading to improvements in ExE [11]. In what follows, we take advantage of this composite mirror layer structure to further integrate photonic nanoantenna arrays capable of influencing the radiation from the MQWs.

Figure 10 summarizes the various photonic phenomena that embedded nanostructures can induce either simultaneously or individually. Depending on their fundamental nature, we may classify them in terms of far-field or near-field tailoring.

- Bragg reflection: It is based on one-dimensional DBR structures, as shown in the diagram of Figure 11. As demonstrated in the Drexhage experiment [14], this composite reflector can affect the emission properties of the active region leading to the ability of controlling the LDOS [15]. Enhancements in both Purcell factor and angular emission characteristics originate from a set of Fabry-Perot resonances appearing in the layer stack.
- Grating Diffraction: Bragg reflection is combined with diffraction gratings in order to further leverage radiation enhancement. Nanostructures as shown in Figure 11 may or may not be in close proximity to the active region as the design is tailored to optimize the far-field angular radiation.
- Surface Lattice Resonance (SLR): The metasurface consists of resonant nanoparticles made of metal supporting localized surface plasmon resonance (LSPRs), i.e. coherent oscillation of electrons in the nanoparticles. Similar effects can be obtained with dielectrics, such as TiO2 embedded in SiO2, which support Mie resonances. Arrays of nanoparticles acting as nanoantennas may support collective plasmonic resonances known as surface lattice resonances (SLRs), which are the result of the enhanced radiative coupling between the resonances of the individual nanoparticles through in-plane diffraction orders known as Rayleigh anomalies (RAs). A characteristic of SLRs is that they support high near-field enhancements, which are weakly confined to the individual

nanoparticles. This enhancement can reach sufficient distance from the individual nanoparticles, enabling the desired coupling to the MQWs. In order to exploit this phenomena, nanoantennas are located on the surface of the TCO layer (e.g. Indium Tin Oxide, ITO) and subsequently embedded in a high refractive index layer (e.g. TiO2) that index matches with that of GaN (see Figure 11), thereby maximizing the coupling to the MQWs. A low-refractive-index layer may separate the metasurface layer from the back metallization layer and further promote upward radiation into the LES.

- Quasi-Guided Modes (QGM): Similarly to SLR, waveguides can be tailored to support guided modes with slow decaying fields that allow radiative energy coupling from evanescence fields emitted by the MQWs. These guided modes can be made radiative by the integration of scattering structures, such as grating couplers. The directions of radiation can be further steered by means of the geometry of the grating. Figure 11 shows a possible implementation of the concept.

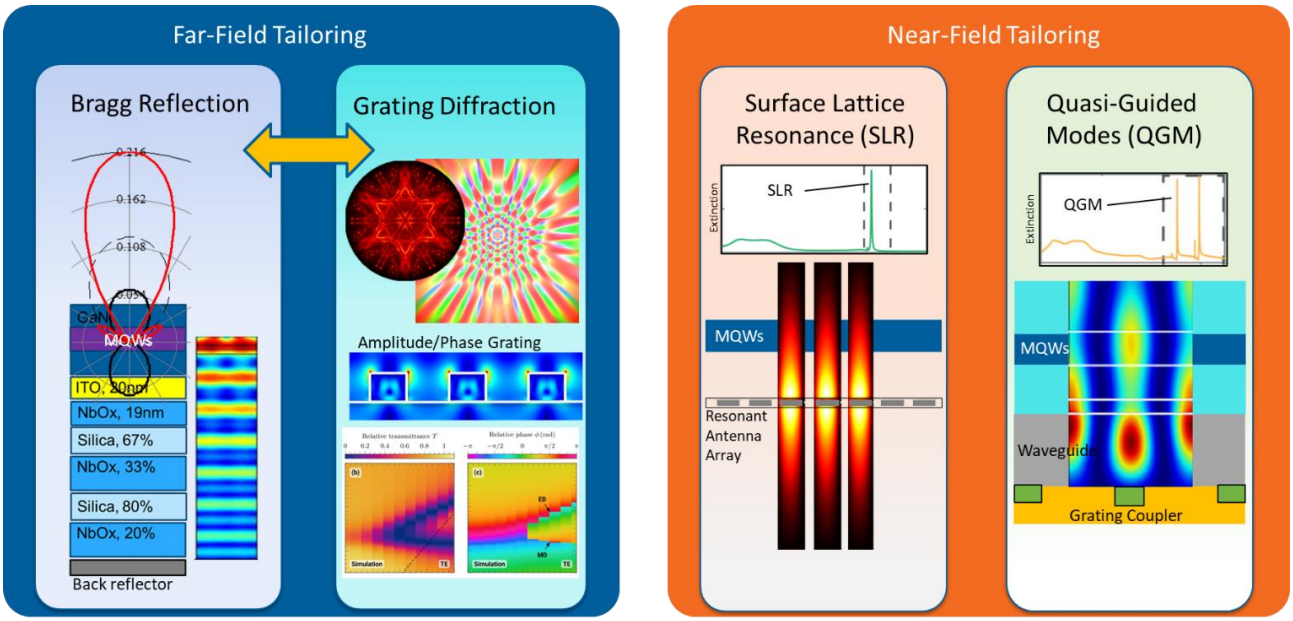

Figure 10. Classification of photonic phenomena in metasurface composite mirror reflectors for LEDs.

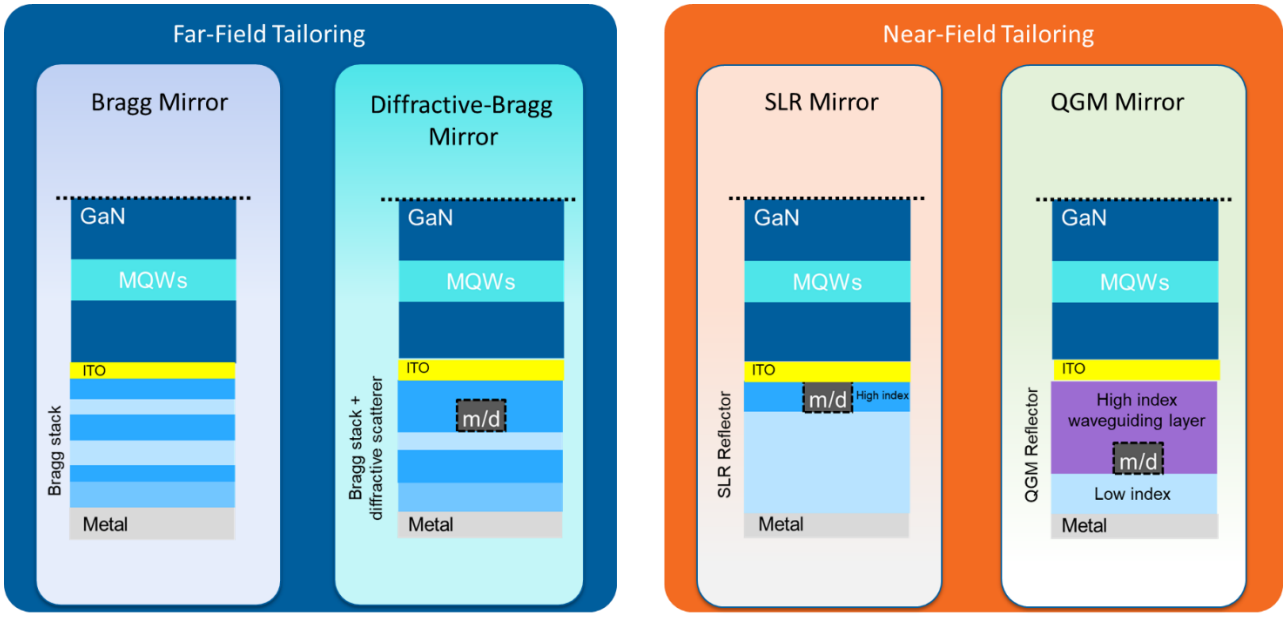

Figure 11. Classification of metasurface composite mirrors for LED devices. Note that only the unit cell is represented for lateral periodic structures. The top LES of the LED is omitted. Note m/d means metal or dielectric nanoparticles.

Through a benchmark and down-selection process, we studied, designed, and optimized the above candidate structures showing the highest potential benefits in terms of fabrication feasibility and device performance. Among the selected designs, we fabricated samples with different Al nanodisk metasurfaces deposited onto an InGaN/GaN green LED sapphire wafer coated with a thin 20nm ITO layer. The nanoantenna array was subsequently covered with a Nb2O5 layer [16]. The schematic representation of the sample is shown in Figure 12. Using Fourier microscopy, we characterized the angular-resolved far-field emission I(θ,ϕ) from the MQWs integrated with the Al-based metasurfaces, also shown in Figure 12 along with model projections. Here, the MQWs were excited by a continuous-wave (CW) laser emitting at 405nm. The sample was illuminated from the sapphire side at normal incidence. These experiments allowed us to quantitatively validate the influence of the SLRs on the outcoupled emission.

Further investigations focused on benchmarking integrated plasmonic versus all-dielectric metasurfaces, and therefore we designed the structures shown in Figure 13. The optimized spatial dimensions for each case point out the difference in feature sizes given the clearly distinct scattering strengths between metal and dielectric nanoparticles. Nonetheless, both designs could render significant forward-beaming shapes as the far-field diagrams highlight. The radiation enhancement as a function of solid-angle collection was quantified relative to the Lambertian emission of an optimized planar microLED design assuming negligible side-wall effects. Results presented in Figure 14 suggest that plasmonic losses prevent superior performance despite the scattering strength advantages of the metallic nano-particles. On the other hand, the low-loss all-dielectric design offers 3x gains at 20deg half-cone angle and 2x at 45deg.

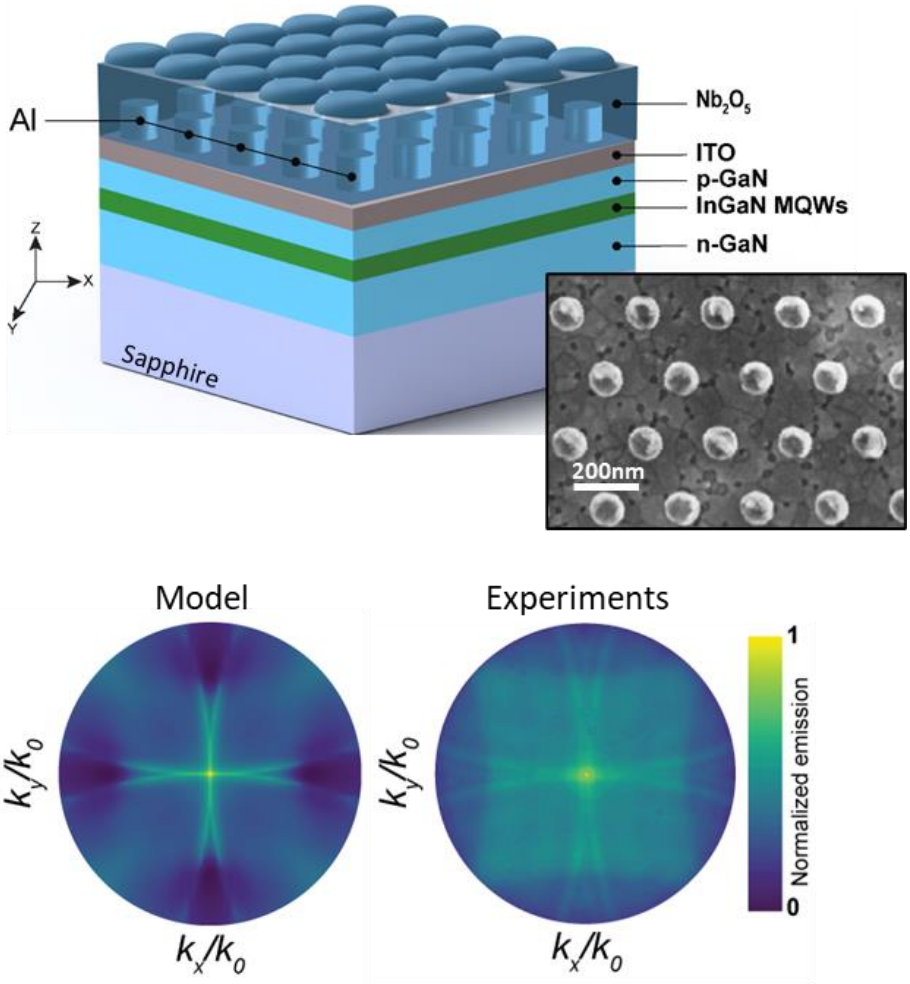

Figure 12. Investigated sample description. (Top) Al metasurfaces placed on a GaN LED wafer and covered by a layer of Nb2O5. The laser emission (λ = 405 nm) illuminating the sample from the sapphire side excites the InGaN MQWs, which emit at 570 nm. Inset: SEM top view of the Al nanodisks (with 55nm height). (Bottom) Measured and simulated back focal plane (BFP) image at λ = 570 nm. The BFP image has a radius of 0.9, which corresponds to the numerical aperture (NA) of the objective in the setup. Images from [16].

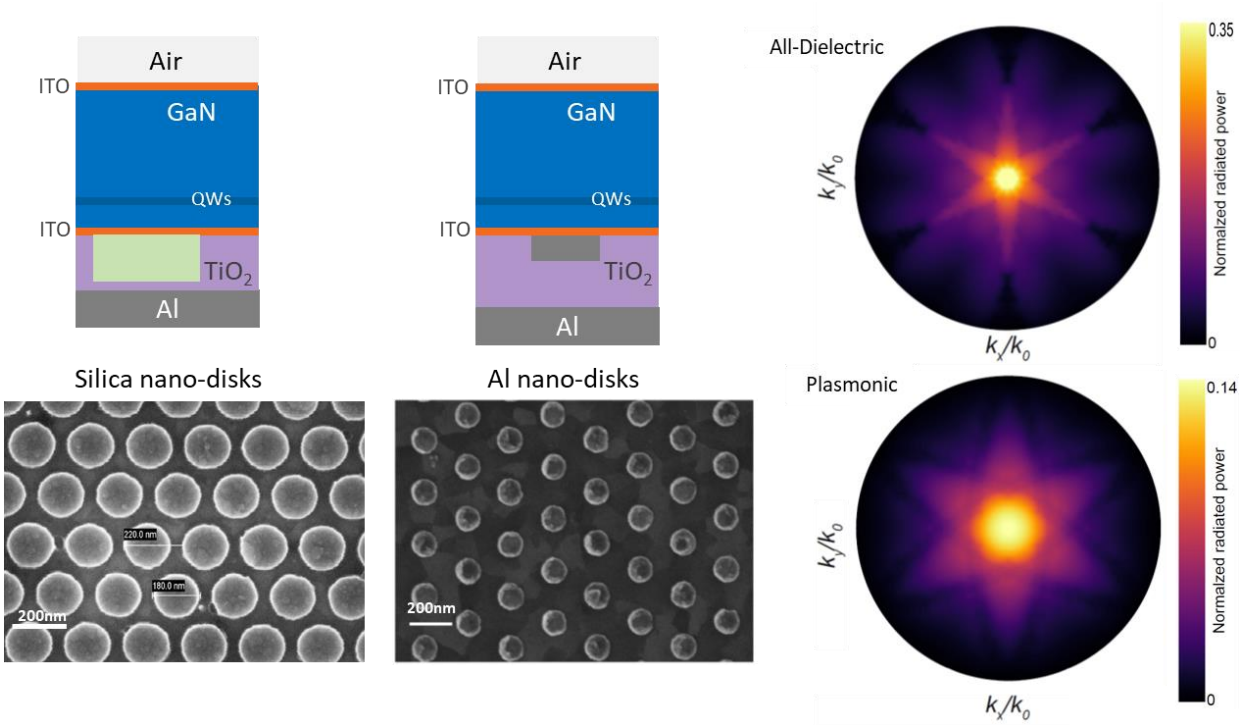

Figure 13. Integrated plasmonic vs. all-dielectric metasurface composite mirror designs and their corresponding (simulated) angular radiation characteristics in k-space. Feature heights vary between 50nm and 100nm depending on the optimization target. Note green color in cross-sectional figure represents a silica nanoparticle.

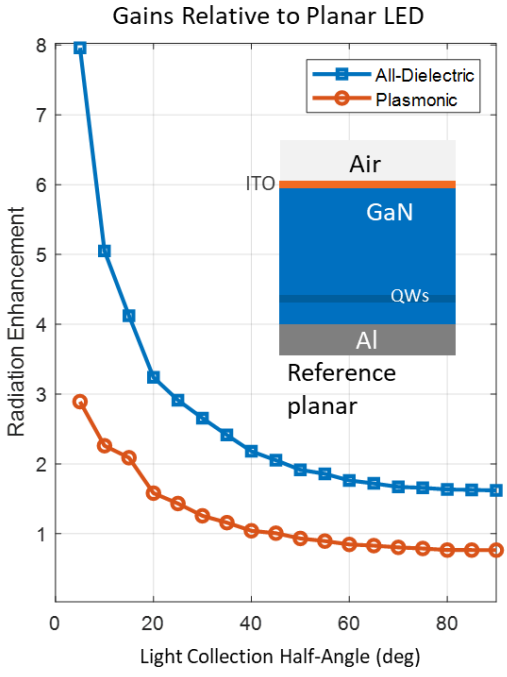

Figure 14. Simulated radiation enhancement as a function of light collection angle for the designs in Figure 13. Gains are relative to an optimized planar microLED design with negligible side-wall effects.

Taking the all-dielectric metasurfaces as a preferential choice, we conducted further studies on improved designs suitable for microLEDs, as shown in Figure 15. In contrast to previous designs, the additional oxide layer can improve reflectance while maintaining similar beam-steering capabilities. With comparable nanoparticle dimensions, Figure *16* shows that the resulting forward-beam profile can couple light efficiently within a half-cone angle of 30deg. Relative to the reference planar design, the radiation enhancement when ignoring side-wall effects increases approximately by 4x at the same collection angle and roughly by 3x at 90deg. Compared to the planar composite mirror design with conventional textured LES (see dashed red line in lower plot of Figure *16*), the metasurface-based design remains more efficient for collection half-angles below 40deg.

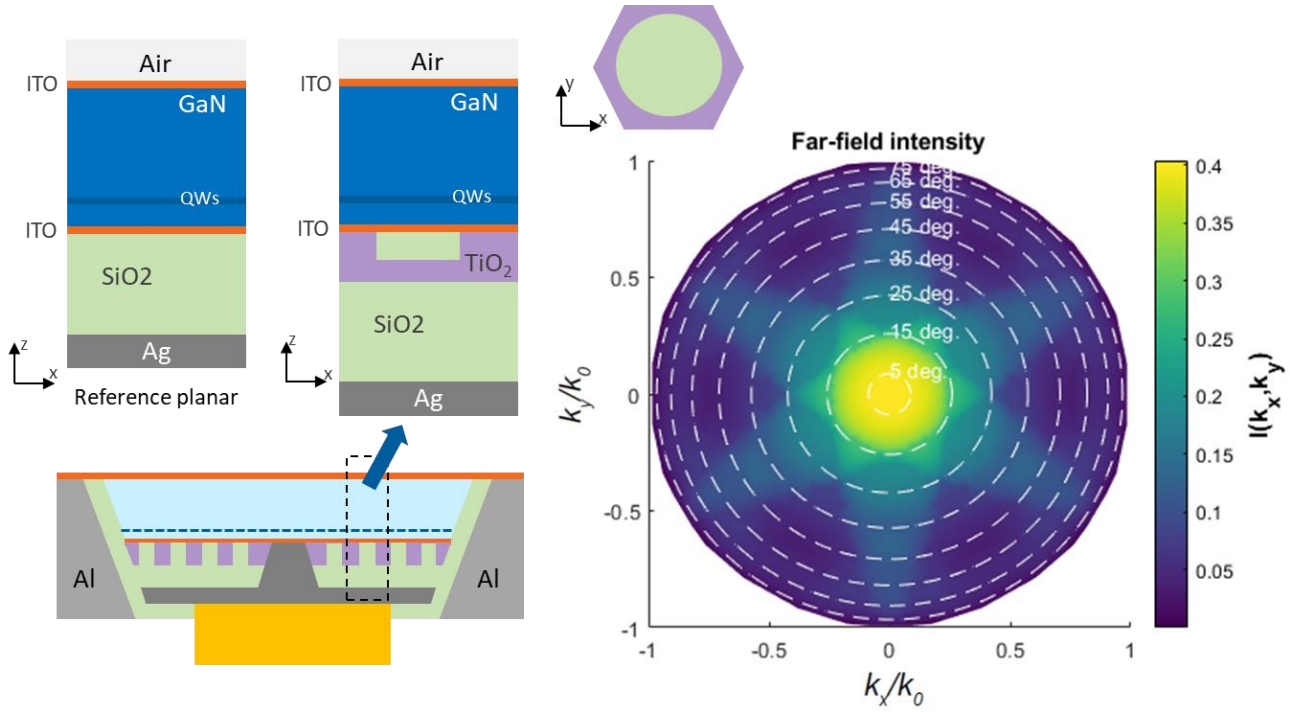

Figure 15. (Left) Integrated all-dielectric metasurface composite mirror of a microLED and reference planar design. (Right) Simulated far-field intensity in k-space corresponding to an optimized metasurface composite mirror design.

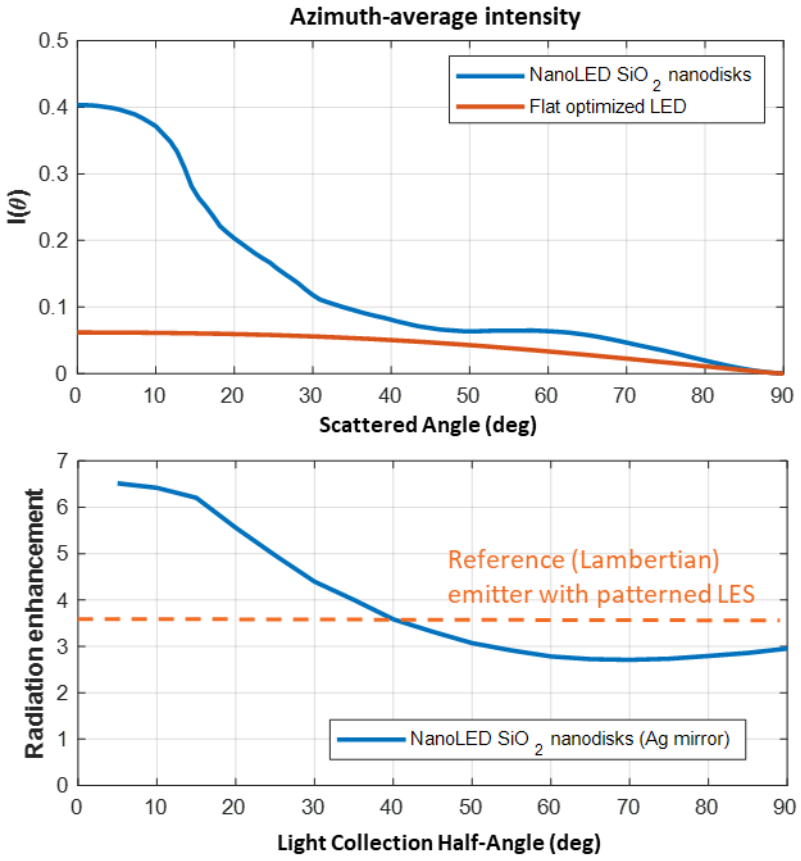

Figure 16. Simulated angular radiation characteristics (top) and radiation enhancement (bottom) corresponding to the designs in Figure 15. The flat LED refers to the reference planar design, which renders Lambertian radiation. Dashed line corresponds to the improved case of the flat LED with textured LES.

A relevant question to address in the microLED design concerns the requirements in number of nano-structure periods necessary to avoid subdiffraction lattice limits. Therefore, numerical simulations were conducted to obtain the far-field emission pattern for the μLED device integrated with a finite metasurface array, varying the number of periods. Figure 17 shows the configurations included, i.e. (a) a single metasurface particle, (b) 2 periods, (c) 4 periods, (d) 6 periods, (e) 8 periods, and (f) an infinite Al-based metasurfaces array. The calculated emission values were relative to the power emitted by the dipoles placed in a homogeneous and infinitely extended layer of GaN. The far-field plots demonstrate that strong collimation begins with a minimum number of six periods. In combination with the resulting lattice dimensions at each color wavelength, we can readily establish a lower bound microLED size limit of approximately 2-4μm for the effectiveness of this type of metasurfaces.

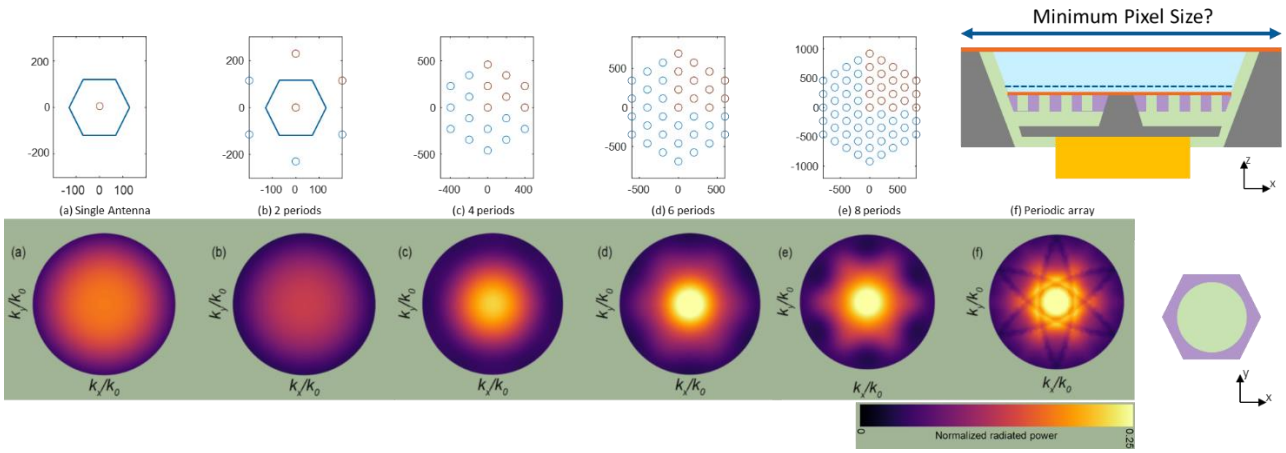

Figure 17. The minimum pixel size dependence on the minimum required lattice periods of the nanostructure lattice array.

5. CONCLUSIONS

LED technology is evolving and tailored to meet the demands of modern applications. Examples include adaptive LEDs for local dimming in AR displays and the rapid progress recently reported in microLEDs with regards to materials, device performance, architectures, and reliability. Associated key performance metrics include efficient directional beaming in order to reduce volume size of secondary optics while keeping low power consumption in battery-driven portable devices. This calls for viable microLED architectures whose optical performance may be significantly affected not only by pixel size but also by associated manufacturing process complexities. Surface photonics are proposed as solutions to enable both directional control of angular emission and radiation enhancement in a compact form factor. In this study, we demonstrate the following benefits and challenges of various photonic structures integrated in LED devices:

- Package level metalens integration: We demonstrate proper lens operation in combination with a distributed light source (i.e. a direct-color adaptive LED emitter), but lateral size and outcoupling efficiency remain challenging due to high angle collection requirements and material absorption, particularly in the blue band.
- PhC/Diffractive nano-structures: Nano-PSS offers feasible efficient beaming capabilities in comparison to previous PhC device architectures of higher complexity.
- Metasurface composite mirrors: These offer compact integration in close proximity to the active region, which allows for highly effective light manipulation.

All-dielectric metasurfaces fabricated with industry-standard materials have potential as integral building block of next-generation direct-color LEDs of sizes down to the micrometer scale.

6. REFERENCES

[1] E. Young and others, "Segmented Red, Green, and Blue Light Sources for Energy Efficient LCoS AR Displays," *Proceedings SPIE,* 2024.

[2] B. Moran and others, "Progress in MicroLEDs: Materials, Device Performance, and Reliability," *Proceedings SPIE,* 2024.

[3] L. Baruah, "MicroLED Microdisplays: An Invention Fueled by AR," *information display.org,* 2022.

[4] J. Flemish, "Development and Industrialization of InGaN/GaN LEDs on Patterned Sapphire Substrates for Low Cost Emitter Architecture," *U.S. Department of Energy,* 2015.

[5] O. Shchekin and others, "High performance thin-film flip-chip InGaN–GaN light-emitting diodes," *Applied Physics Letters,* vol. 89, no. 071109, 2006.

[6] J. Flemish and others, "MicroLED architectures for low power wearable displays," *Proceedings SPIE 12022, Light Emitting Devices, Materials and Applications XXVI,* no. 1202203, 2022.

[7] L. Annaniah and others, "LED Packaging Technologies: Design, Manufacture, and Applications," *Wiley,* 2023.

[8] J. Wierer and others, "III-nitride photonic-crystal light-emitting diodes with high extraction efficiency," *Nature Photonics 3,* pp. 163-169, 2009.

[9] J. Wierer and others, "InGaN/GaN quantum-well heterostructure light-emitting diodes employing photonic crystal structures," *Applied Physics Letter,* pp. 3885-3887, 2004.

[10] M. Ohya and others, "LED Element," *US Patent 9634188B2,* 2017.

[11] A. Tandon and others, "Strategies for better brighter LED's," *Compound Semiconductor,* vol. 23, no. 2, 2017.

[12] E. Lopez and others, "Tripling the light extraction efficiency of a deep ultraviolet LED using a nanostructured p-contact," *Nature Scientific Reports,* vol. 12, no. 11480, 2022.

[13] Y.-C. Shen and others, "Optical cavity effects in InGaN/GaN quantum-well-heterostructure flip-chip light emitting diodes," *Applied Physics Letters,* vol. 82, no. 14, pp. 2221-2223, 2003.

[14] K. Drexhage, "Influence of a dielectric interface on fluorecence decay time," *Journal of Luminescense,* Vols. 1-2, pp. 693-701, 1970.

[15] H.-Y. Ryu, "Investigation of the purcell effect in GaN-based vertical LED structures using FDTD simulation," *Optical and Quantum Electronics,* vol. 48, 2015.

[16] M. S. Abdelkhalik and others, "Surface lattice resonances for beaming and outcoupling green μLEDs emission," *Nanophotonics - De Gruyter,* vol. 12, no. 18, pp. 3553-3562, 2023.

7. ACKNOWLEDGMENTS

Authors would like to thank the following students and postdoctoral researchers at TU/e: Dr. Aleksandr Vaskin, Dr. Anton Matthijs Berghuis, Thomas-Jan van Raaij and Lianne M.A. de Jong for all their support and valuable contributions. Likewise, we wish to express our gratitude to Prof. Femius Koenderink and his PhD student Deba Pal from AMOLF for their valuable feedback during our regular discussions. Finally, we would like to thank the Dutch Research Council (NWO) for their financial support.